Systems/Circuits

Neural Correlates of Personal Space Intrusion

Daphne J. Holt,[1,2,3] Brittany S. Cassidy,[4] Xiaomin Yue,[5] Scott L. Rauch,[2,6] Emily A. Boeke,[1,3] Shahin Nasr,[3,7] Roger B. H. Tootell,[2,3,7] and Garth Coombs III[1,3]

[1]Department of Psychiatry, Massachusetts General Hospital, Boston, Massachusetts 02114, [2]Harvard Medical School, Boston, Massachusetts 02115, [3]Athinoula A. Martinos Center for Biomedical Imaging, Charlestown, Massachusetts 02129, [4]Department of Psychology, Brandeis University, Waltham, Massachusetts 02453, [5]National Institute of Mental Health, Bethesda, Maryland 20892, [6]McLean Hospital, Belmont, Massachusetts 02478, and [7]Department of Radiology, Massachusetts General Hospital, Boston, Massachusetts 02114

A parietal-frontal network in primates is thought to support many behaviors occurring in the space around the body, including interpersonal interactions and maintenance of a particular "comfort zone" or distance from other people ("personal space"). To better understand this network in humans, we used functional MRI to measure the responses to moving objects (faces, cars, simple spheres) and the functional connectivity of two regions in this network, the dorsal intraparietal sulcus (DIPS) and the ventral premotor cortex (PMv). We found that both areas responded more strongly to faces that were moving toward (vs away from) subjects, but did not show this bias in response to comparable motion in control stimuli (cars or spheres). Moreover, these two regions were functionally interconnected. Tests of activity-behavior associations revealed that the strength of DIPS-PMv connectivity was correlated with the preferred distance that subjects chose to stand from an unfamiliar person (personal space size). In addition, the magnitude of DIPS and PMv responses was correlated with the preferred level of social activity. Together, these findings suggest that this parietal-frontal network plays a role in everyday interactions with others.

Key words: **connectivity; fMRI; intraparietal sulcus; personal space; premotor cortex; social behavior**

Introduction

Like eye gaze and facial expression, personal space plays an important role in communication with others. Although personal space is influenced by state and situation-dependent variables, such as the degree of familiarity of the interacting individuals (Hayduk, 1983), there is some evidence for a trait-like "optimal distance" which varies between individuals, but is somewhat stable following adolescence (Hayduk, 1983; Bar-Haim et al., 2002). Although this behavior has been well described, the neural mechanisms that influence personal space characteristics have been little studied.

Electrophysiological studies in nonhuman primates suggest that the space around the body is represented and monitored by a network of parietal and frontal regions (Graziano and Cooke, 2006). Neurons in a multisensory region within the fundus of the intraparietal sulcus, the ventral intraparietal area (VIP), respond preferentially to objects that are in "near space" (<20 cm from the body), particularly the space around the head (Colby et al., 1993; Duhamel et al., 1998). Interestingly, some VIP neurons respond to moving objects in a direction-selective manner, responding best to stimuli moving toward the head or body (Colby et al., 1993). Similar responses have also been reported for a subset of single units in a multisensory region within the ventral premotor cortex (PMv; Fogassi et al., 1996; Graziano et al., 1997), an area that receives afferents from VIP but not from adjacent parietal regions (Luppino et al., 1999).

Functional MRI studies conducted in humans have identified areas with multisensory and/or near-space preferring responses in parietal (Bremmer et al., 2001; Sereno and Huang, 2006; Makin et al., 2007; Quinlan and Culham, 2007; Swisher et al., 2007; Silver and Kastner, 2009; Brozzoli et al., 2011) and frontal (Bremmer et al., 2001; Brozzoli et al., 2011) cortex. However, it is not known whether these parietal and frontal areas in human brain are particularly responsive to stimuli that are "looming" toward (approaching, vs withdrawing from) the head or body. Here we used functional MRI to test for such a response bias to known objects (socially relevant (faces) and nonsocially relevant (cars)) in a region surrounding the dorsal intraparietal sulcus (DIPS; Orban et al., 2003) and the ventral PMv. We also compared the magnitude of looming responses to the faces and cars, to determine whether the social relevance of the stimuli influenced these responses. For the car and face stimuli, the size of the objects was familiar; thus, the subject could infer the distance of the object from the observer. To control for this effect of inferred size, we also measured fMRI activity in response to unfamiliar spheres, in which the objective size of the stimulus cannot be inferred. To distribute attention evenly across the conditions, subjects performed a dummy attention task while viewing the stimuli. In addition, we tested for evidence of neural connections between these areas (Luppino et al., 1999), using resting-state functional connectivity methods. Finally, we deter-

Received Feb. 13, 2013; revised Dec. 30, 2013; accepted Jan. 22, 2014.

Author contributions: D.J.H., S.L.R., and R.B.H.T. designed research; D.J.H., B.S.C., X.Y., S.N., and G.C. performed research; D.J.H., B.S.C., E.A.B., and G.C. analyzed data; D.J.H., R.B.H.T., and G.C. wrote the paper.

This study was supported by the National Institute of Mental Health K23MH076054 (DH).

The authors declare no competing financial interests.

Correspondence should be addressed to Dr Daphne J. Holt, 149 13th Street, Charlestown, MA 02129. E-mail: dholt@partners.org.

DOI:10.1523/JNEUROSCI.0686-13.2014

 0270-6474/14/344123-12$15.00/0

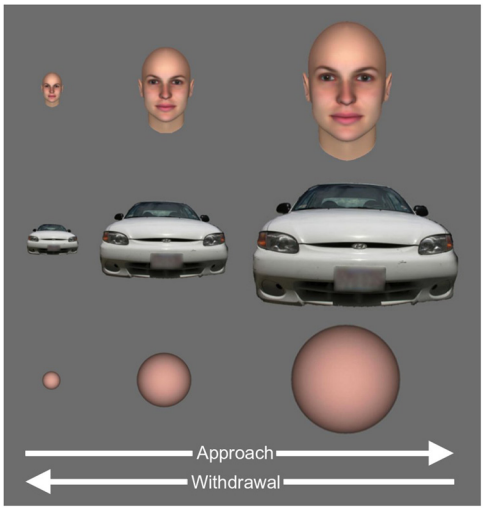

Figure 1. Experimental stimuli. Examples of each of the stimuli types used in the study (computer-generated human faces, photos of cars, and computer-generated spheres) are shown.

mined whether interindividual variation in the activity and functional connectivity of DIPS and PMv is related to personal space size.

Materials and Methods

Participants

Eight healthy subjects (mean age ± SD = 26.4 ± 4.7 years; 4 males) were initially enrolled in the study. An additional 14 subjects (mean age ± SD = 24.6 ± 4.5 years; 8 males) were later enrolled, to provide additional power to examine associations between fMRI activity and social behavior. This second group of subjects was scanned using a slightly modified version of the paradigm (see Stimuli, below). All subjects were American-born (ethnicity: 16 Caucasian non-Hispanic subjects, 2 Caucasian-Hispanic, 1 Asian-American, 2 African-American).

MRI data acquisition

Two anatomical 3D MPRAGE scans (256 coronal slices spatial resolution 3 mm isotropic, TR = 2530 ms, TE = 3.39 ms, flip angle = 7°) and 10 functional runs (each 256 s in duration; TR = 2000 ms, TE = 30 ms, flip angle = 90°; 33 axial slices; 128 images per slice, 3 mm isotropic voxels) were collected on a 3T Siemens Tim Trio scanner. For a subset of the subjects ($n = 17$), one 6 min and 20 s resting BOLD scan (TR = 5000 ms; TE = 30 ms; flip angle = 90°; 55 axial slices; 76 images per slice, 2 mm isotropic voxels) was also acquired, during which subjects were instructed to keep their eyes open and blink normally.

Stimuli

*Paradigm 1 (*n = *8).* During each functional run, subjects viewed three types of stimuli that either expanded or contracted (i.e., appearing to approach or withdraw from the subject). Stimuli were human faces with neutral emotional expressions, cars, and spheres. Each of the six conditions (Face Approach, Face Withdrawal, Car Approach, Car Withdrawal, Sphere Approach, Sphere Withdrawal) was presented for 16 s at a time (Fig. 1). Two 16 s fixation blocks were presented at the beginning and end of each run. In each run, subjects viewed two blocks of each of the six conditions, randomly presented. The minimum stimulus size was 3.1° × 3.1° and the maximum stimulus size was 17.2 ° × 17.2 °. The stimuli changed in size, appearing to approach or withdraw, at a rate equivalent to a speed of 112 cm/s (2.5 mph), a typical walking speed. The stimuli consisted of three male faces, three female faces, eight cars, and eight spheres. The faces were created with FaceGen (http://www.facegen.com), a program used to create realistic human faces.

*Paradigm 2 (*n = *14).* This was identical to Paradigm 1 except that the sphere stimuli were omitted. Thus, two blocks of each of four conditions were presented during each run.

Table 1. Personal space size and permeability

Subject	Experimenter	Personal space size (cm) D1	Personal space size (cm) D2	Personal space permeability
Male	Male	58.6 ± 38.5	28.3 ± 21.9	58.4 ± 17.9%
	Female	53.6 ± 23.6	19.4 ± 12.3	68.9 ± 15.5%
Female	Male	68.2 ± 25.0	30.8 ± 13.5	55.6 ± 8.9%
	Female	52.0 ± 21.2	23.4 ± 11.9	55.7 ± 9.5%

Average personal space sizes (Distance 1, D1) and personal space permeability (mean ± SD) of the male ($n = 10$) and female ($n = 10$) subjects in response to male and female experimenters as determined by the Stop Distance Paradigm (see Materials and Methods) are listed. Distance 2 (D2) is used to calculate the permeability of personal space.

Task

To distribute spatial attention evenly across the Approach and Withdrawal conditions, subjects were asked to press a button, while maintaining fixation, whenever a dot appeared at a random location on the screen. Five dots appeared per 16 s block, randomly timed between 980 ms and 1980 ms. The duration of the dot stimulus varied from 500 ms to 1500 ms, and dot size varied with eccentricity. The percentage of responses was calculated for each condition, for each subject.

MRI data analysis

Data were analyzed using the FreeSurfer analysis stream (http://surfer.nmr.mgh.harvard.edu). Because the location of approach-preferring areas of the dorsal parietal and ventral premotor cortices was not known a priori, initially an unbiased anatomical region-of-interest (ROI) analysis was conducted. The boundaries of the DIPS and PMv ROIs were defined in each subject using an automated parcellation method (FreeSurfer) that uses anatomical landmarks to define borders between cortical gyri and sulci (Fischl et al., 2004). The dorsal borders of the superior parietal gyrus parcellation were used to delineate the dorsal portion of DIPS, which roughly corresponds to the motion-sensitive portion of the dorsal parietal lobe surrounding the intraparietal sulcus (Orban et al., 2003). The dorsal border of the superior occipital gyrus and the superior and transverse occipital sulcus was used to define the ventral boundary of the DIPS ROI. PMv was defined as the ventral portion of the precentral gyrus parcellation. The dorsal border of PMv was defined by the ventral border of the superior precentral sulcus parcellation. All fMRI data of one subject and one run of three subjects were excluded from the fMRI analyses because of low response rates during the dot-detection task (responded to <40% of trials). One fMRI run of one subject was excluded due to excessive head motion (>2 mm).

Primary analysis: anatomical ROI. A repeated-measures ANOVA [2 (region: DIPS, PMv) × 2 (hemisphere: left, right) × 2 (condition: Approach, Withdrawal) × 3 (stimuli type: faces, cars, spheres)] was conducted to test for a main effect and/or interactions with condition in the initial cohort of subjects ($n = 8$). A modified version of this ANOVA (with 2 stimuli types: faces and cars) was used to test for similar effects in the full cohort of subjects ($n = 21$). Lastly, to test for main effects or interactions with gender (subject or stimulus) in an exploratory analysis, an ANOVA that also included terms for stimulus and subject gender (male, female) was used.

Secondary, follow-up analysis: cortical surface-based. To localize any effects found with the ANOVA and to test for approach-biased activity outside of the two predefined ROIs, functional data were also sampled onto the cortical surface and projected onto an average spherical representation. The contrasts of interest (Approach − Withdrawal, for each condition), and contrasts testing for interactions between condition (Approach, Withdrawal) and stimulus type (Faces, Cars, Spheres), were tested using a *t*-statistic at each vertex on the spherical surface using random effects. Clusters of activated vertices are reported if they met a significance threshold of $p < 0.05$ corrected for the False Discovery Rate (FDR) and a size threshold of 10 mm^2.

Functional connectivity analyses. Standard preprocessing techniques for resting-state functional connectivity analyses (Buckner et al., 2009) were used to selectively capture variance in the BOLD signal corresponding to low-frequency (<0.08 Hz) fluctuations in neural activity during the resting-state. Nuisance regressors, including the six parameters com-

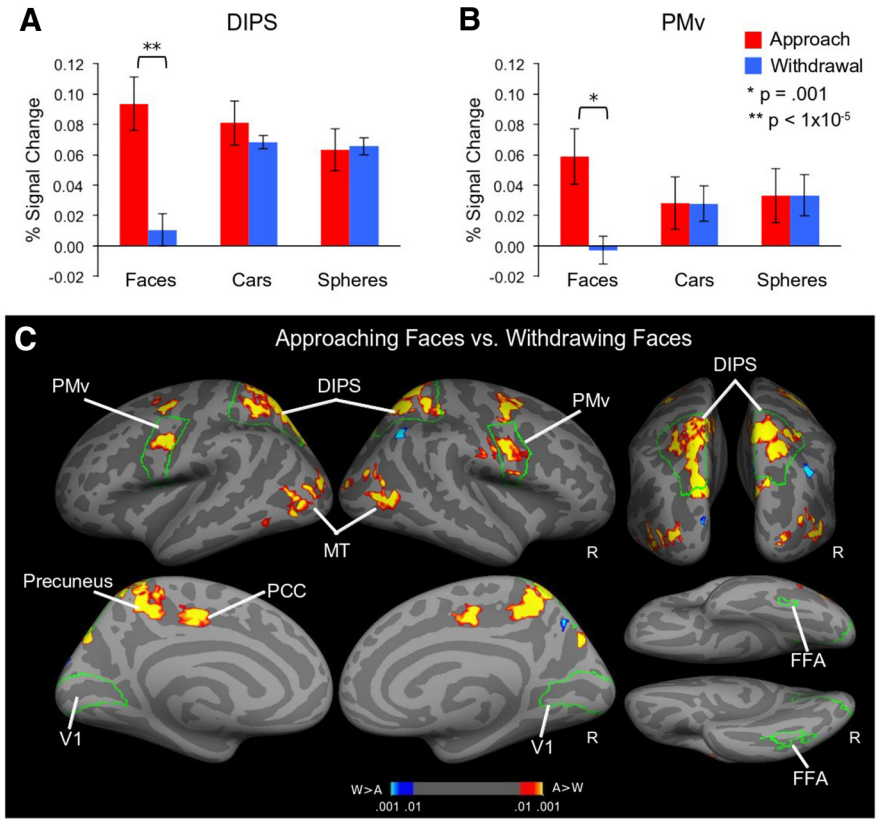

Figure 2. Functional MRI responses to approaching and withdrawing faces, cars, and spheres. The results of the analysis conducted using the DIPS (***A***) and PMv (***B***) anatomical ROIs are shown ($n = 8$). DIPS and PMv show a significant approach bias to faces, but not to cars or simple spheres. ***C***, Lateral, medial, superior, and inferior views of cortical surface maps of activation to Approaching versus Withdrawing faces in the full cohort ($n = 21$) are shown. The outlines of the anatomically defined DIPS and PMv ROIs are shown in green, as well as the outlines of primary visual cortex (V1; defined as the region around the calcarine sulcus activated to all stimuli compared with fixation, at a height threshold of $p < 0.05$) and the FFA (defined as the region in the fusiform gyrus activated to all face stimuli compared with all car stimuli, at a height threshold of $p < 0.05$). These maps reveal that although DIPS and PMv show approached-biased responses, as well as a number of other regions, such as the PCC, precuneus, dorsal premotor cortex, and MT, lower-level visual areas, such as V1 and FFA, do not show this bias; Table 2, top. W, Withdrawal; A, Approach; R, right.

puted from the rigid-body motion correction, the averaged signal within a ventricular ROI, a region within the deep white matter, and the signal averaged over the whole brain, were used to remove systematic variance associated with these variables. The first temporal derivative of each regressor was also included to account for temporal shifts in the BOLD signal.

To create whole-brain correlation images for DIPS and PMv, the averaged time series across all voxels comprising a seed (i.e., voxels within right and left DIPS or PMv showing any activation ($p < 0.05$) for the main contrast, see Results) was used as the variable of interest in a linear regression with the time series corresponding to each voxel across the brain. The statistical analyses of these correlational data were performed on Fisher *z*-transforms (Zar, 1996). Group-level functional connectivity maps (one sample *t* tests, random effects) were constructed using SPM5 (http://www.fil.ion.ucl.ac.uk/spm) and clusters which met a threshold of $p < 0.05$, FDR corrected, >10 voxels in size, were considered significantly correlated with the seed.

Before testing for a correlation between personal space size and DIPS-PMv connectivity, the DIPS and PMv seed regions were further constrained to the voxels within the DIPS and PMv ROIs with the strongest intercorrelated activity (i.e., the most specific network for this cohort). Thus, the voxels within the PMv ROI showing connectivity to DIPS constituted a seed that was used to identify voxels within the DIPS ROI with the strongest correlations with PMv. We tested our primary behavioral hypotheses, that (1) DIPS or PMv activation or (2) DIPS-PMv connectivity was correlated with personal space size, using Spearman's ρ with α set at $0.05/2 = 0.025$.

Secondary voxelwise multiple-regression analyses, using the behavioral measures as effects of interest, were also conducted, using the DIPS seed, to test for associations between the behavioral measures and DIPS-PMv and DIPS-default network connectivity. For these analyses, correlations meeting a threshold of $p < 0.01$ uncorrected and ≥ 10 voxels in size are reported. Lastly, the results of additional exploratory correlational analyses involving the behavioral measures are reported using an α of 0.05 uncorrected.

These additional correlational analyses were conducted to provide convergent evidence for any relationship found between frontoparietal function/connectivity and social behavior (i.e., if correlations between neural activity and several measures of social behavior are detected, the likelihood of Type 1 statistical error is diminished).

Measurements of personal space size and levels of social activity

Outside of the scanner, personal space size was measured in all subjects using the Stop-Distance Paradigm (Kaitz et al., 2004), a validated method for measuring personal space size with high reliability ($\kappa \sim 0.8$; Hayduk, 1983). This procedure includes the following steps: an experimenter and the subject begin by standing 3 m apart. The experimenter slowly walks toward the subject, maintaining a neutral facial expression. Before the procedure, the subject had been instructed to say "O.K." when he/she feels "slightly uncomfortable," i.e., when his/her personal space ("the typical distance you stand away from someone you have never met before") has been entered. The experimenter notes this distance as the subject's personal space size (Distance 1; D1). After D1 is measured, the experimenter resumes walking toward the subject. The subject says, "O.K." again when he/she feels "very uncomfortable" (Distance 2; D2). The ratio of D1 and D2 [$100 - (D2 \times 100)/D1$] indicates the subject's ability to tolerate personal space intrusion (the "permeability" of personal space). This procedure is then repeated with a second experimenter of the opposite gender. The order of the two experimenters (male or female first) is counter-balanced across subjects. Two personal space measures were examined here: personal space size (D1) and permeability.

To test for effects of gender on personal space size and permeability, a 2×2 (experimenter gender × subject gender) ANOVA was conducted for each outcome, followed by *t* tests.

The personal space data of one subject was omitted from the analyses because he did not follow the task instructions. Another subject did not have personal space size measurements for a male experimenter.

On the day of scanning, subjects also filled out a questionnaire that asked them to estimate the average percentage of their waking hours spent with other people versus alone, and the percentage of their waking hours that they would prefer to spend with other people versus alone.

Results

Behavior

Personal space size

Across all subjects, mean personal space size (D1) was 60.5 ± 5.3 cm (Table 1). Mean personal space permeability was 58.2 ±

Table 2. Functional MRI responses to approaching and withdrawing faces and cars ($n = 21$)

Region	BA	Hemi	Tal (x, y, z)	Size (mm^2)	Z	p
A. Faces Approach versus Faces Withdrawal contrast						
Approach > Withdrawal						
Precuneus	7	R	11, −44, 51	291.1	5.6	3×10^{-8}
	7	L	−8, −44, 54	155.5	4.8	2×10^{-6}
Superior parietal gyrus (dorsal)[a]	7	L	−19, −70, 40	553.7	5.3	1×10^{-7}
	7	R	10, −53, 57	397.8	5.2	2×10^{-7}
	7	R	25, −51, 52	191.2	4.3	2×10^{-5}
	7	R	35, −41, 57	80.4	4.3	2×10^{-5}
	7	L	−17, −57, 59	60.5	4.3	2×10^{-5}
	7/2	R	30, −33, 44	14.6	3.9	1×10^{-4}
	7/5	L	−34, −44, 56	87.1	3.9	1×10^{-4}
	7	L	−12, −52, 56	20.0	3.7	2×10^{-4}
	7/5	L	−22, −47, 57	15.6	3.7	2×10^{-4}
	7	L	−23, −51, 61	17.0	3.6	3×10^{-4}
Mid-cingulate gyrus	24	L	−14, −17, 41	69.6	4.6	5×10^{-6}
	24	R	14, −13, 38	54.6	4.2	3×10^{-5}
	24	L	−13, −16, 35	12.1	3.5	5×10^{-4}
Precentral gyrus (dorsal); middle frontal gyrus	4	R	37, −4, 44	138.2	4.5	8×10^{-6}
	6	R	23, 5, 44	14.0	3.9	1×10^{-4}
	6	L	−31, −1, 41	54.2	3.7	2×10^{-4}
Superior parietal gyrus (ventral)	7	R	20, −73, 35	79.6	4.4	1×10^{-5}
	7	R	24, −69, 41	33.5	4.3	2×10^{-5}
Precentral gyrus (ventral)[b]	6	L	−51, −3, 27	35.9	4.0	7×10^{-5}
	6	L	−55, −2, 35	48.7	3.7	2×10^{-4}
	6	R	52, −3, 29	108.6	3.7	2×10^{-4}
Middle occipital gyrus, inferior temporal gyrus	18	L	−30, −87, 15	50.8	4.0	7×10^{-5}
	37	R	45, −71, 7	64.8	4.0	7×10^{-5}
	19	R	40, −76, 20	13.3	3.7	2×10^{-4}
	37	L	−40, −73, 4	23.2	3.7	2×10^{-4}
Withdrawal > Approach						
Inferior parietal gyrus, supramarginal gyrus	40	R	45, −58, 42	46.6	3.7	2×10^{-4}
B. Faces Approach − Withdrawal versus Cars Approach − Withdrawal contrast						
Superior parietal gyrus (dorsal)[a]	7	R	11, −53, 57	202.0	4.7	3×10^{-6}
	7	R	35, −41, 56	56.9	4.3	2×10^{-5}
	7	R	19, −58, 51	26.1	4.2	3×10^{-5}
	7	R	30, −33, 44	24.0	3.9	1×10^{-4}
	7	R	25, −51, 52	14.8	3.7	2×10^{-4}
Precuneus	7	R	12, −44, 55	114.8	4.1	5×10^{-5}
Superior frontal gyrus	6	R	22, 4, 44	10.9	4.0	7×10^{-5}
Precentral gyrus (ventral)[b]	6	R	54, −1, 24	43.0	3.9	8×10^{-5}
Precentral gyrus (dorsal), middle frontal gyrus	6	R	38, −4, 45	46.8	3.9	9×10^{-5}
Superior parietal gyrus (ventral)	7	R	24, −69, 41	11.2	3.9	1×10^{-4}
Middle, inferior temporal gyri	39	R	42, −64, 11	24.9	3.7	2×10^{-4}
Postcentral gyrus	43	R	61, −11, 24	14.3	3.6	3×10^{-4}

A, Clusters are listed which showed significantly ($p < 0.05$, FDR corrected, cluster size threshold >10 mm^2) greater activation to Approaching versus Withdrawing face stimuli, as well as one cluster in the inferior parietal cortex showing greater activation to Withdrawing, compared with Approaching, faces ($n = 21$). B, Clusters are listed which showed a significantly greater approach bias (Approach > Withdrawal) to face compared to car stimuli ($n = 21$). No cluster showed a greater approach bias to cars compared with faces. Clusters falling within the predefined anatomical regions-of-interest (DIPS, PMv) are indicated with *a* and *b* (*a*, DIPS; *b*, PMv). Figs. 2, 3. Note that although the peak activations shown at the bottom are in the right hemisphere only, this is because the FDR threshold was higher for the left than for the right hemisphere (because of overall higher levels of activation in the right (vs the left hemisphere). At a non-FDR corrected threshold ($p < 0.0005$, cluster size >20 mm^2), there is activation for this contrast in both the left (−18, −72, 43; $z = 4.5$; $p = 7 \times 10^{-6}$; 88 mm^2) and right (11, −53, 57; $z = 4.7$; $p = 3 \times 10^{-6}$; 213 mm^2) DIPS and left (−52, −3, 28; $z = 4.4$; $p = 1 \times 10^{-5}$; 97 mm^2) and right (54, −1, 24; $z = 3.9$; $p = 8 \times 10^{-5}$; 47 mm^2) PMv. BA, Brodmann area; Hemi, hemisphere; Tal, Talaraich coordinates of peak vertex; L, left; R, right.

2.1%. These values are similar to those previously reported (Hayduk, 1981).

Social activity

Subjects reported spending an average of 61.1 ± 6.1% of their waking hours with others, and preferred to spend a similar amount of their waking hours with others (64.1 ± 5.5%).

DIPS and PMv activity

Anatomical ROI analysis

Responses of DIPS and PMv to faces, cars and spheres that were moving toward ("Approaching") or away from ("Withdrawing") participants were first measured in eight subjects. An ANOVA revealed a significant interaction between condition and stimulus type ($F_{(2,14)} = 12.2$, $p = 1 \times 10^{-3}$) with no condition by stimulus type by hemisphere interaction ($F_{(2,14)} = 1.54$, $p = 0.25$), reflecting a significantly larger response to Approaching (compared with Withdrawing) faces in both DIPS ($t_{(7)} = 8.0$, $p < 1 \times 10^{-3}$) and PMv ($t_{(7)} = 5.3$, $p < 1 \times 10^{-3}$; Fig. 2*A*,*B*). However, DIPS and PMv responses to the car and sphere stimuli did not show this approach bias ($t < 1.1$; $p > 0.26$). A second cohort of subjects ($n = 13$) was then tested using only the face and car stimuli. When the ANOVA was repeated in the full cohort ($n = 21$; excluding the sphere control condition), the results were similar to those of the initial analysis. We found a significant condition by stimuli type interaction ($F_{(1,20)} = 9.8$, $p = 5 \times 10^{-3}$) with no interaction with hemisphere ($F_{(1,20)} = 1.06$, $p = 0.32$), reflecting a significantly larger response to Approaching (vs Withdrawing) faces in DIPS ($t_{(20)} = 3.9$, $p = 1 \times 10^{-3}$) and PMv ($t_{(20)} = 3.0$, $p =$

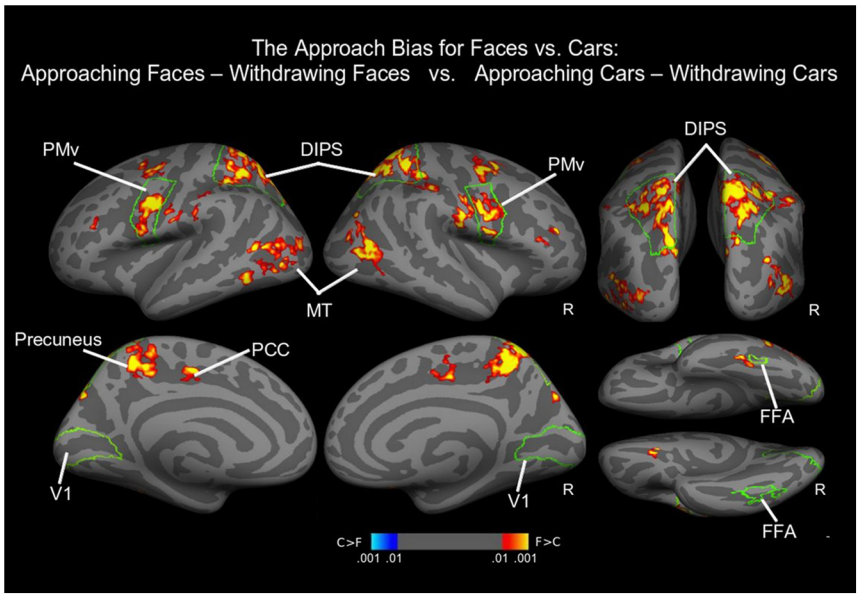

Figure 3. The approach bias to faces compared with the approach bias to cars. This figure shows the results of the analysis conducted using the following contrast: (Approaching − Withdrawing Faces) − (Approaching − Withdrawing Cars) in the full cohort ($n = 21$) in lateral, medial, superior, and inferior views of cortical surface maps. DIPS and PMv show a significantly greater approach bias to faces, compared with cars. The outlines of the anatomically defined DIPS and PMv ROIs are shown in green, as well as the outlines of V1 and the FFA; Table 2B. W, Withdrawal; A, Approach; R, right; C, approach-biased responses to the car stimuli; F, approach-biased responses to the face stimuli.

8×10^{-3}). Again, DIPS and PMv responses to the car stimuli did not show this approach bias (DIPS: $t_{(20)} = 0.3$, $p = 0.80$; PMv: $t_{(20)} = 1.0$, $p = 0.33$).

Follow-up, cortical surface-based analysis

Cortical surface maps of the Approach versus Withdrawal responses for each stimulus type, in both the initial and full (Table 2) cohorts, confirmed the findings of the anatomical ROI analyses. Greater responses to Approaching versus Withdrawing faces were seen in DIPS and PMv, as well as in the precuneus, mid cingulate gyrus, dorsal precentral and middle frontal gyri, middle occipital and inferior temporal gyri, and ventral superior parietal gyrus (Fig. 2*C*; Table 2A). No significant differences were found between responses to Approaching and Withdrawing cars in DIPS, PMv, or elsewhere in the cortex. Thus the approach-biased response (Approach > Withdrawal) was significantly greater to faces compared with cars in both DIPS and PMv (Fig. 3; Table 2B). Moreover, in the smaller cohort of subjects, the approach-biased responses were greater to faces compared with cars and spheres in DIPS (left: Talairach coordinates x, y, z: −16, −68, 45; $z = 4.4$, $p = 1 \times 10^{-5}$; right: 10, −55, 57; $z = 4.8$, $p = 2 \times 10^{-6}$) and PMv (left: −48, 3, 16; $z = 4.2$, $p = 3 \times 10^{-5}$; right: 51, 8, 26; $z = 3.6$; $p = 3 \times 10^{-4}$).

In addition, there were no differences in responses to Approaching and Withdrawing faces in primary visual cortex or in the Fusiform Face Area (Figs. 2*C*, 3). This suggests that this direction bias was not simply due to a greater tendency of the subjects to attend to the Approaching (vs Withdrawing) faces.

Consistent with this pattern of results was the absence of differences between the two conditions or for any of the stimulus types in response rates for the dot-detection task performed during the scans (i.e., no main effect of condition or condition by stimulus type interaction, all $F < 2.7$; $p > 0.12$). This suggests that there were no differences between the two conditions in the level of attention allocated to the stimuli.

Functional connectivity of approach-biased DIPS and PMv

Resting-state BOLD activity of the DIPS seed (which was constrained to the voxels within the DIPS ROI showing greater responses to Approaching versus Withdrawing faces at $p < 0.05$) correlated significantly with activity of a ventral portion of the anatomically defined PMv ROI (Fig. 4; Table 3). In addition, activity of a similarly constrained PMv seed was correlated with activity of an anterior portion of the DIPS ROI. An additional analysis revealed that the portion of PMv with significant connectivity with the DIPS seed (Fig. 4*A*; see Materials and Methods) also showed strong connectivity with the dorsal portion of DIPS (Fig. 5). In addition, strong inverse (anti-) correlations were found between resting BOLD activity of DIPS and PMv and regions of the default network, i.e., medial prefrontal, posterior cingulate, lateral temporal and parietal cortices (Fig. 4; Table 3), consistent with previous connectivity findings for frontoparietal circuits involved in monitoring external space (Fox et al., 2005, 2006; Yeo et al., 2011). Thus, the DIPS-PMv network demonstrates the expected connectivity pattern of the larger "dorsal attention system" (Fox et al., 2005; Vincent et al., 2008), with strong connectivity within a network that represents external space and anti-correlations with a network involved in attending to "inner space" (i.e., introspection).

Correlations with behavior

Correlations between personal space and social activity measures

Personal space permeability was correlated with the amount of time subjects spent with others ($r = 0.46$; $p = 0.04$) and the amount of time subjects preferred to spend with others ($r = 0.47$; $p < 0.04$). In addition, there was a trend toward an inverse correlation between personal space size (D1) and the amount of time subjects spent with others ($r = -0.39$; $p = 0.09$).

Correlations between approach-biased DIPS and PMv responses and behavior

There were no correlations between personal space size (or personal space permeability) and approach-biased activation of DIPS or PMv. However, approach-biased responses of the right and left DIPS and left PMv correlated with the amount of time participants preferred to spend with others (left DIPS: $r = 0.52$, $p < 0.02$; right DIPS: $r = 0.52$, $p < 0.02$; left PMv: $r = 0.43$, $p < 0.05$; trend for the right PMv: $r = 0.37$, $p = 0.096$).

Correlations between the strength of DIPS-PMv functional connectivity and behavior

The strength of DIPS-PMv functional connectivity (measured using seeds limited to the areas of DIPS and PMv with the strongest intercorrelated activity, see Materials and Methods; Fig. 5) was negatively correlated with personal space size ($r = -0.55$, $p = 0.02$; Fig. 6*B*). That is, weaker DIPS-PMv functional coupling was associated with a requirement for increased personal space. In this conservative ROI-based analysis, DIPS-PMv connectivity did not correlate with other behavioral measures

Table 3. Functional connectivity of DIPS and PMv ($n = 17$)

Region	BA	Hemi	Tal (x, y, z)	Size (voxels)	Z	p_c
DIPS functional connectivity						
Positive correlations						
Superior parietal gyrus (dorsal)	7	L	−24, −53, 63	23737	7.1	$<1 \times 10^{-4}$
Precentral gyrus (dorsal), middle frontal gyrus	4/6	R	34, −4, 46	1249	4.8	$<1 \times 10^{-4}$
	4/6	L	−30, −5, 46	880	4.7	1×10^{-4}
Precentral gyrus (ventral)	6	L	−51, 7, 25	617	4.7	1×10^{-4}
	6	R	51, 8, 11	994	4.1	5×10^{-4}
Fusiform gyrus, cerebellum	37	R	26, −53, −12	397	4.4	2×10^{-4}
Middle frontal gyrus	9	R	40, 42, 29	359	4.4	2×10^{-4}
	9	L	−38, 40, 27	99	3.7	2×10^{-3}
Cerebellum		L	−50, −50, −34	35	4.3	3×10^{-4}
		R	46, −50, −31	89	3.9	1×10^{-3}
		R	28, −73, −22	18	3.3	7×10^{-3}
Pericalcarine, lingual gyri	17	R	2, −87, 6	45	3.5	4×10^{-3}
	17	R	2, −75, 9	64	3.0	2×10^{-2}
Inferior frontal gyrus	45/46	R	40, 31, 6	51	3.3	6×10^{-3}
	45	L	−32, 28, 12	35	3.2	9×10^{-3}
Middle cingulate gyrus	24		0, 9, 29	25	3.1	1×10^{-2}
Negative (anti-) correlations						
Hippocampus, parahippocampal gyrus	27	L	−20, −22, −11	24934	5.7	9×10^{-4}
Superior temporal gyrus	22	L	−59, −48, 21	1570	5.2	1×10^{-3}
	39	R	55, −59, 23	935	4.3	2×10^{-3}
Middle temporal gyrus	22	L	−46, −12, −1	257	4.2	2×10^{-3}
		L	−30, 9, −6	41	3.7	5×10^{-3}
Middle frontal gyrus	6	R	20, 22, 58	119	3.9	4×10^{-3}
	8	L	−40, 16, 49	273	3.7	5×10^{-3}
Inferior frontal gyrus	45	L	−50, 24, 12	57	3.3	1×10^{-2}
	45	R	57, 32, 9	13	2.9	2×10^{-2}
Cerebellum		R	57, −60, −27	11	3.3	1×10^{-2}
		L	−10, −34, −20	16	3.1	2×10^{-2}
Inferior temporal gyrus	20	L	−63, −21, −23	13	3.0	2×10^{-2}
PMv functional connectivity						
Positive correlations						
Precentral gyrus, middle frontal gyrus	6/4	L	−51, −4, 32	36231	7.3	$<1 \times 10^{-4}$
Temporal pole	38	L	−24, 12, −33	155	4.1	6×10^{-4}
	38	L	−40, 20, −23	17	2.9	2×10^{-2}
Inferior frontal gyrus	45	R	53, 35, 4	65	3.7	2×10^{-3}
Middle cingulate gyrus	31	L	−14, −18, 38	56	3.7	2×10^{-3}
	31/5	R	16, −26, 45	53	3.2	9×10^{-3}
Caudate		R	2, 10, 7	78	3.6	2×10^{-3}
Middle temporal gyrus	21/37	L	−51, −56, 6	117	3.6	3×10^{-3}
	37	R	51, −58, −2	54	3.3	6×10^{-3}
Thalamus		L	−10, −19, 1	32	3.4	5×10^{-3}
		R	14, −20, 18	10	3.1	1×10^{-2}
Superior temporal gyrus	36	R	16, 4, −29	103	3.4	5×10^{-3}
Amygdala		R	22, −1, −18	21	3.2	7×10^{-3}
Superior parietal gyrus (dorsal)	7	L	−18, −63, 60	57	3.2	8×10^{-3}
Fusiform gyrus	37	L	−44, −51, −11	11	3.0	1×10^{-2}
Negative (anti-) correlations						
Precuneus, posterior cingulate gyrus	31	L	−10, −59, 29	9338	5.3	3×10^{-3}
Inferior parietal gyrus, angular gyrus	19/39	R	46, −70, 37	1959	4.7	3×10^{-3}
Superior parietal gyrus	19/30	L	−38, −70, 40	1192	4.6	3×10^{-3}
Medial frontal gyrus	10		0, 58, 1	2352	4.5	3×10^{-3}
Inferior temporal gyrus	37	L	−63, −49, −14	885	4.5	3×10^{-3}
	20	R	65, −37, −10	42	3.6	9×10^{-3}
Fusiform gyrus	20	R	46, −18, −18	476	4.4	3×10^{-3}
Lingual gyrus, pericalcarine sulcus	18	R	4, −80, −1	300	4.3	3×10^{-3}
	17	L	−28, −69, 13	13	3.4	1×10^{-2}
Middle frontal gyrus	6	R	20, 20, 54	501	4.3	4×10^{-3}
	10	L	−26, 60, −1	12	3.0	3×10^{-2}
	8	R	40, 16, 42	32	3.0	3×10^{-2}
	8	L	−28, 11, 33	34	3.3	2×10^{-2}
Caudate		R	16, 9, 18	68	3.8	6×10^{-3}
Putamen		L	−14, 2, −2	19	3.8	6×10^{-3}

Table continued

Table 3. *Continued*

Region	BA	Hemi	Tal (*x*, *y*, *z*)	Size (voxels)	*Z*	p_c
Thalamus		L	−24, −27, 5	28	3.8	6×10^{-3}
Cerebellum		L	−20, −45, −47	44	3.7	7×10^{-3}
		R	26, −41, −38	10	3.6	1×10^{-2}
		L	−24, −40, −30	24	3.1	2×10^{-2}
		R	51, −50, −27	15	3.1	2×10^{-2}
		L	−34, −85, −24	14	3.0	3×10^{-2}
Lateral orbitofrontal gyrus	11	R	38, 36, −17	115	3.7	7×10^{-3}
Rostral anterior cingulate gyrus	32	L	−16, 47, 3	24	3.3	2×10^{-2}
Uncus	38	R	30, 9, −16	33	3.3	2×10^{-2}
Medial orbitofrontal gyrus	10		0, 50, −16	47	3.3	2×10^{-2}
Brain stem		R	10, −31, −34	18	3.2	2×10^{-2}
Parahippocampal gyrus	36	R	24, −17, −26	21	3.1	2×10^{-2}
Superior frontal gyrus	9	L	−22, 44, 35	11	2.8	4×10^{-2}

Clusters showing significant connectivity ($p < 0.05$, FDR corrected; cluster size threshold $>10\,mm^2$) with the DIPS (top) and PMv (bottom) seed regions are listed ($n = 17$). BA, Brodmann area; Hemi, hemisphere; Tal, Talaraich coordinates of peak voxel; L, left; R, right.

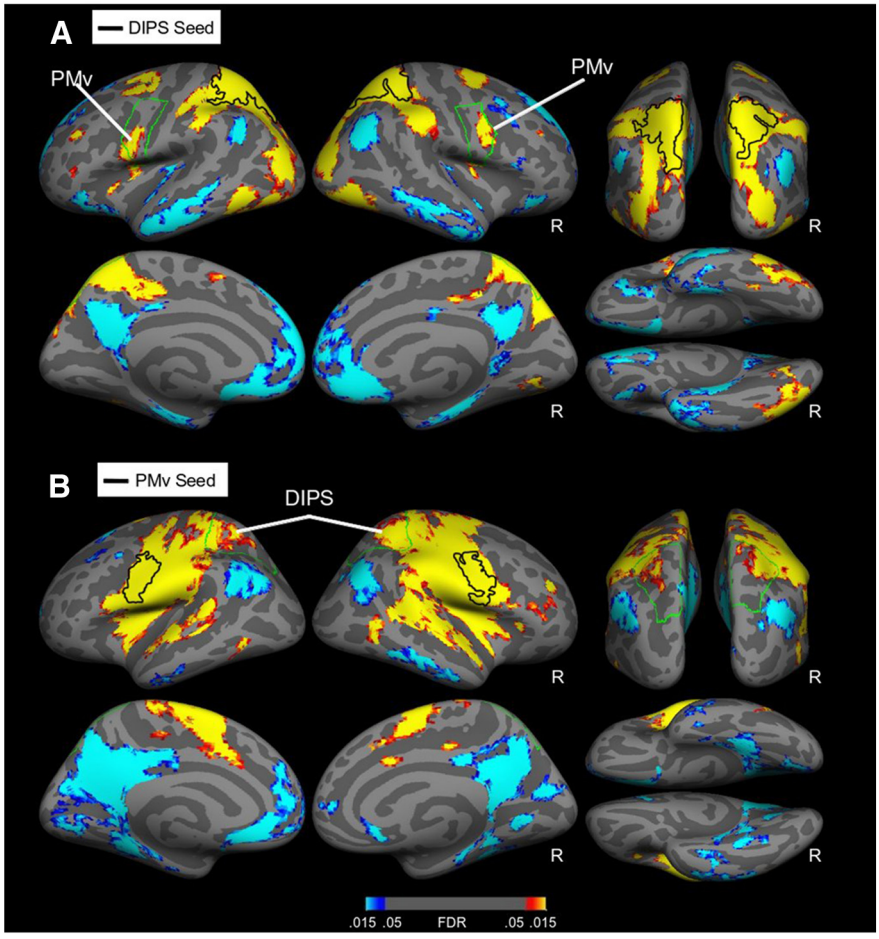

Figure 4. Functional connectivity of approach-biased DIPS and PMv. Clusters showing significant connectivity ($p < 0.05$; FDR corrected, cluster size threshold $> 10\,mm^2$) with the DIPS (***A***) and PMv (***B***) seed regions (which were constrained to voxels showing significant ($p < 0.05$) activation to the Approaching versus Withdrawing face stimuli) are displayed on inflated cortical surface maps ($n = 17$). Clusters showing positive correlations with the seed are shown in yellow-red, whereas those showing negative (anti-) correlations with the seed are shown in blue. In each panel, the seed is outlined in black, whereas the hypothesized target area for that seed (anatomically defined DIPS or PMv; see Materials and Methods) is outlined in green and labeled; Table 3. R, Right.

(personal space permeability, percentage of time spent with others), although there was a trend toward a positive correlation between DIPS-PMv functional coupling and the amount of time participants preferred to spend with others ($r = 0.43$, $p = 0.08$).

In a secondary, voxelwise analysis, these same relationships were examined using whole brain regression and functional connectivity of the DIPS seed. Again the strength of DIPS-PMv functional coupling was found to be negatively correlated with personal space size ($z = 3.4$; $p = 3 \times 10^{-4}$; Fig. 6*C*; Table 4). In addition, positive correlations were found between DIPS-PMv coupling and personal space permeability ($z = 3.6$; $p = 2 \times 10^{-4}$; Fig. 6*D*; Table 4), and also between DIPS-PMv coupling and both actual ($z = 3.4$, $p = 3 \times 10^{-4}$) and preferred ($z = 3.8$, $p = 1 \times 10^{-4}$) percentage of time spent with others (Fig. 6*E*,*F*; Table 4). Thus, greater DIPS-PMv coupling predicted lower personal space size and greater personal space permeability. In other words, increased coupling of these regions was linked with less discomfort with physical proximity to others, as well as greater levels of preferred and actual social activity.

Finally, the strength of functional coupling between DIPS and regions of the default network (which are normally anti-correlated; Fig. 4) was positively correlated with personal space size, and negatively correlated with personal space permeability (Fig. 7). Thus, consistent with the results described above for the connectivity between DIPS and PMv, stronger anti-correlations between DIPS and the default network predicted lower personal space size and increased personal space permeability (i.e., greater comfort with physical proximity to others).

Additional (control) analyses

When these correlational analyses were repeated using DIPS and PMv ROIs defined by the contrast used in Figure 3 (the approach bias for faces vs cars), similar results were found, i.e., a significant negative correlation was detected between DIPS-PMv connectivity and personal space size ($r = -0.55$; $p = 0.02$).

Personal space size, permeability, and social activity measures did not correlate with head motion parameters, age or IQ (all $p > 0.27$).

Gender effects

We also measured the effects of subject gender and the gender of the face stimuli on our outcome measures. We found that personal space size was greater in response to male than to female experimenters ($t_{(18)} = 2.9, p = 0.01$) during the Stop Distance Paradigm. That is, subjects preferred to stand further away from males than females, on average. In addition, for male subjects only, personal space permeability was greater in response to female than to male experimenters ($t_{(8)} = 3.1, p < 0.02$), whereas female subjects showed no differences in personal space permeability to male versus female experimenters ($t_{(9)} = 0.02, p = 0.99$).

There were no significant differences between the male and female subjects in the percentage of time preferred or actually spent with others ($t < 0.7; p > 0.52$).

Last, there was a greater approach bias in the fMRI responses to male, compared with female, face stimuli in PMv ($t_{(20)} = 2.3, p = 0.03$) and, at a trend level, in DIPS ($t_{(20)} = 1.9, p = 0.07$).

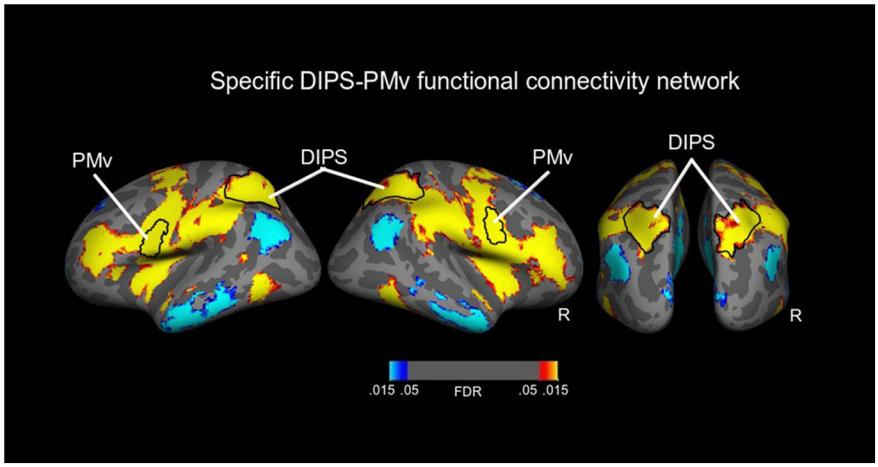

Figure 5. Specific DIPS-PMv functional connectivity network. A PMv seed was derived from the initial DIPS connectivity map (Fig. 4*A*) to isolate the portion of PMv with strong DIPS connectivity (see Materials and Methods). Displayed here is the connectivity map of this PMv seed (the region outlined in black and labeled PMv). Clusters of functionally coupled voxels were deemed significant if they met the following threshold: $p < 0.05$; FDR corrected, size > 10 mm^2. This analysis demonstrates that a ventral portion of the anatomically defined PMv ROI shows strong connectivity with DIPS. The portion of the DIPS ROI showing significant connectivity with this PMv seed is outlined in black and labeled DIPS. R, Right.

Discussion

The first goal of this study was to determine whether there are direction-selective (looming or approach-biased) responses in a parietal-frontal network involved in monitoring peripersonal space, similar to those observed in nonhuman primates. We found that portions of the DIPS region and PMv showed approach-biased responses to face stimuli, but not to cars or spheres. Moreover, these two regions were functionally coupled during a resting state.

A second goal of the study was to test whether this network is functionally linked to habitual social behaviors or traits, such as personal space size and related behaviors. We found that weaker DIPS-PMv functional coupling was associated with having a larger personal space size. Additional analyses revealed that personal space size permeability (the ability to tolerate personal space intrusions) and social activity levels also correlated with DIPS-PMv functional coupling strength. In addition, preferred levels of social activity correlated with approach-biased DIPS and PMv responses to faces. These results suggest that contact with other conspecifics strongly engages this network. Overall, these data support the notion that many social behaviors may not require extensive higher-order cognitive processing; in some instances they can consist of relatively automatic stereotyped actions, coordinated by sensory-motor systems (Graziano, 2009).

An approach-biased frontoparietal network

In VIP and in the polysensory zone of premotor cortex in the monkey, 30–40% of motion- and direction-selective neurons have been reported to respond preferentially to stimuli moving toward, rather than away from, the animal (Colby et al., 1993; Graziano et al., 1997). Also, studies of cells within monkey VIP, or areas within human parietal cortex, have shown response preferences for expanding, as opposed to contracting, optic flow stimuli (Schaafsma and Duysens, 1996; Bremmer et al., 2002; Zhang and Britten, 2004), consistent with an "approach" direction response bias in this network. Accordingly, we tested whether an analogous direction bias can be reliably demonstrated in the human brain, and found that a limited number of frontal and parietal areas show this bias. The area of the superior parietal cortex showing approach-biased responses found here corresponds roughly to previously identified sites within human parietal cortex showing polymodal sensory responses (Bremmer et al., 2001; Sereno and Huang, 2006). For example, a multisensory region of parietal cortex located just posterior to the confluence of the postcentral gyrus and intraparietal sulcus (similar to the location of the approach-biased DIPS region here) has been described previously (Bremmer et al., 2001; Sereno and Huang, 2006; Quinlan and Culham, 2007). This region may also overlap with retinotopically organized areas in anterior parietal cortex, such as IPS4 (Swisher et al., 2007) or IPS5 (Silver and Kastner, 2009). Also, the portion of ventral premotor cortex showing an approach bias here was similar in location to sites reported to have multisensory responses (Bremmer et al., 2001) or responding preferentially to stimuli near the body (Makin et al., 2007; Brozzoli et al., 2011).

However, the exact correspondence of such areas in humans and monkeys remains controversial, because of the greater size of the parietal and frontal lobes in humans compared with monkeys (Orban et al., 2004; Sherwood et al., 2008; Hill et al., 2010). Therefore, we cannot definitively claim that the approach-biased areas identified here in dorsal parietal and ventral premotor cortex represent the human homologues of monkey VIP and PMv. However, this study has revealed only a limited number of human brain areas that show looming responses, which are functionally similar to those reported in a subset of neurons in macaque VIP and PMv.

Although single unit recordings in VIP and PMv in the macaque have shown that some neurons prefer an approaching trajectory of motion compared with a withdrawing one, other neurons are selective for other (e.g., side-to-side; "frontoplanar") directions, and others are not direction-sensitive (Colby et al.,

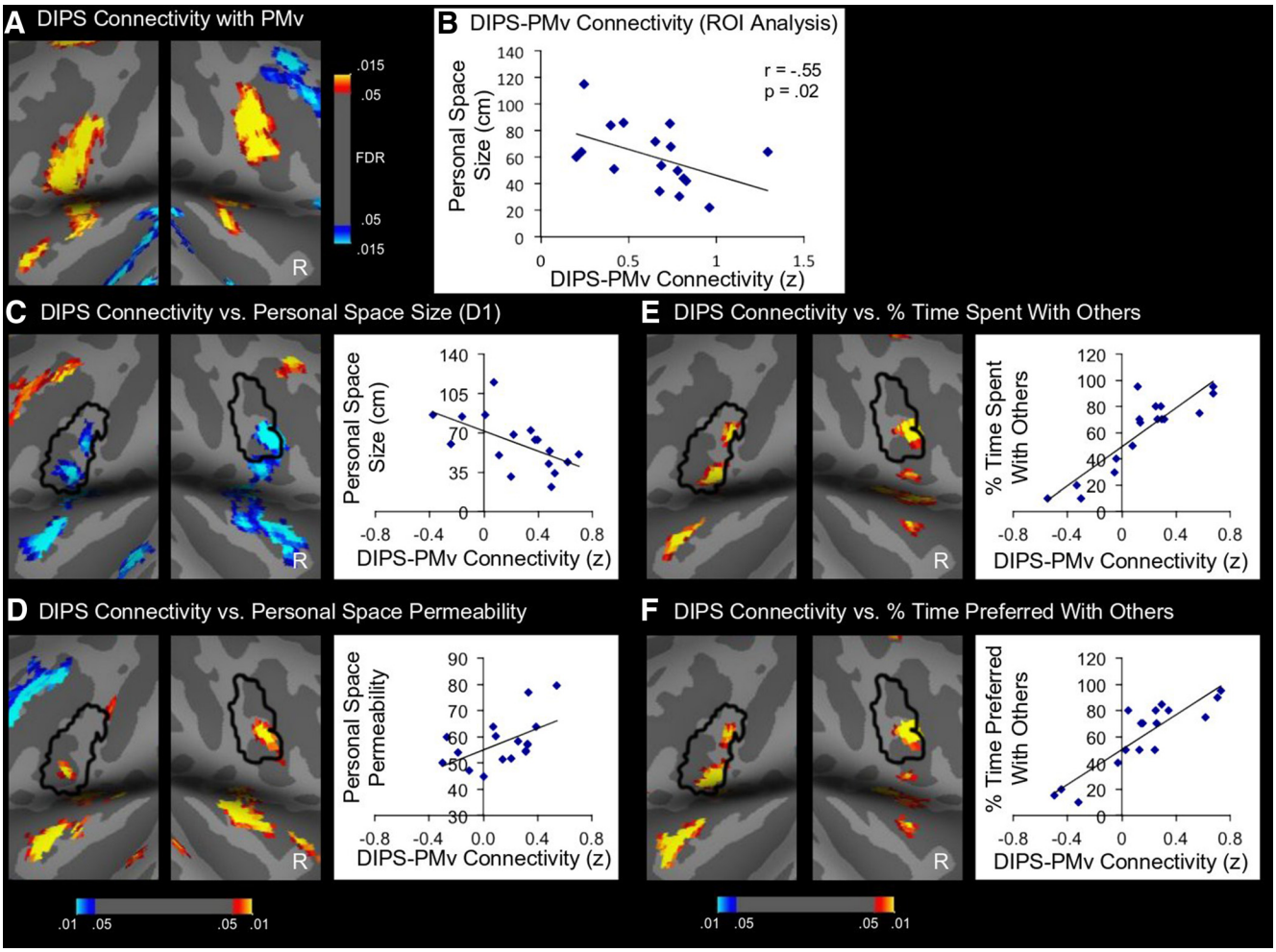

Figure 6. Correlations between DIPS-PMv functional connectivity and behavioral measures. ***A***, Enlarged images of the relevant portions of the DIPS functional connectivity map (see Fig. 4*A*) are shown. An outline of the portion of PMv showing connectivity with DIPS is derived from this map and superimposed on the maps in ***C–F***, to facilitate comparisons. Correlations between DIPS-PMv functional connectivity and behavior were examined by: (1) using predefined DIPS and PMv ROIs to extract the Pearson *r* values representing the degree of DIPS-PMv coupling in each individual (***B***) and (2) conducting voxelwise regression analyses using each behavioral measure as a regressor (***C–F***). ***B***, A scatter plot shows the correlation between DIPS-PMv connectivity and personal space size. ***C–F***, The scatter plots here are derived from the accompanying maps and displayed for illustration purposes only, to show each subject's contribution to the map to the left of each plot. The individual data were extracted using 3 mm radius spherical seeds centered around the two peak correlations in the corresponding map. ***A***, Clusters showing a correlation (positive = yellow-red; negative = blue) with the resting-state activity of the DIPS seed are shown. ***C–F***, Clusters of voxels which show a significant correlation (positive, yellow-red; negative, blue) between the behavioral measure (personal space size, personal space permeability, percentage of time spent with others, and percentage of time preferred with others) and the cluster's connectivity with DIPS are shown ($n = 17$). ***B***, ***C***, DIPS-PMv connectivity is negatively correlated with personal space size. ***D–F***, DIPS-PMv connectivity is positively correlated with personal space permeability, the percentage of time spent with others and the preferred percentage of time spent with others, respectively; Table 4. R, Right; %, percentage.

1993; Graziano et al., 1997). Thus, the regions described here may comprise a network for monitoring a variety of stimuli in peripersonal space including, but not limited to, those that could collide with the body.

It could be argued that our findings reflect a greater allocation of attention to the most behaviorally salient stimuli (face stimuli moving toward the subjects), at least in part. However, several aspects of our results suggest otherwise. First, we controlled for attention variations by using a high-load "dummy" attention task that required subjects to attend equally to the different conditions, across the entire extent of the display screen, throughout scanning. We found no differences in task performance between the Approach and Withdrawal conditions. Second, one would expect that an attention bias to the approaching faces might lead to greater activity in lower-level and ventral visual stream areas, as found in prior studies of volitional attention (Noudoost et al., 2010). However, we did not find any differences between the two conditions in responses of lower-level visual areas, such as V1, or in a face-responsive area, the Fusiform Face Area.

Importantly, symmetrically expanding (relative to contracting) spheres did not produce approach biases in DIPS, PMv, or elsewhere in the brain. A simple, uniformly textured sphere cannot be assigned a location in space because one cannot infer its absolute size from prior knowledge or spatial context. Thus the lack of an approach bias for spheres suggests that knowledge of an object's expected size (which is necessary to judge the speed of the object; Hosking and Crassini, 2010) is required for this bias. Such a requirement would be evolutionarily adaptive, because a size-expanding stimulus is only behaviorally relevant if it is actually moving toward the body. Thus, this result further supports the interpretation that this network is specialized for attending to stimuli that are nearing or entering peripersonal space (Graziano and Cooke, 2006).

Table 4. Correlations between DIPS-PMv functional connectivity and behavior ($n = 17$)

Behavior	BA	Hemi	Tal (x, y, z)	Size (voxels)	Z	p
Positive correlations						
Personal space permeability	4	R	48, 1, 17	168	3.6	2×10^{-4}
	4	L	−48, 2, 7	100	3.2	8×10^{-4}
	6/44	L	−46, 7, 24	12	2.8	3×10^{-3}
Time spent with others	6/44	L	−42, 7, 24	48	3.4	3×10^{-4}
	6	R	53, 4, 11	23	3.2	7×10^{-4}
	6/44	L	−40, 8, 7	18	3.0	2×10^{-3}
Time preferred with others	6/44	L	−44, 7, 24	45	3.8	1×10^{-4}
	6	R	53, 4, 11	43	3.5	2×10^{-4}
	6/44	L	−40, 8, 7	39	3.1	1×10^{-3}
Negative correlations						
Personal space size (D1)	6/44	L	−46, 7, 24	46	3.4	3×10^{-4}
	4	R	48, 1, 17	61	3.1	1×10^{-3}
	6	L	−53, 2, 7	12	2.6	4×10^{-3}

Results are shown of the voxelwise regression analyses of the DIPS functional connectivity data, using each behavioral measure as a regressor. Clusters of voxels within PMv showing a significant ($p < 0.01$, cluster size $> 10\,mm^2$) correlation between the behavioral measure and their connectivity with DIPS are listed ($n = 17$); Fig. 6. BA, Brodmann area; Hemi, hemisphere; Tal, Talaraich coordinates of peak correlation.

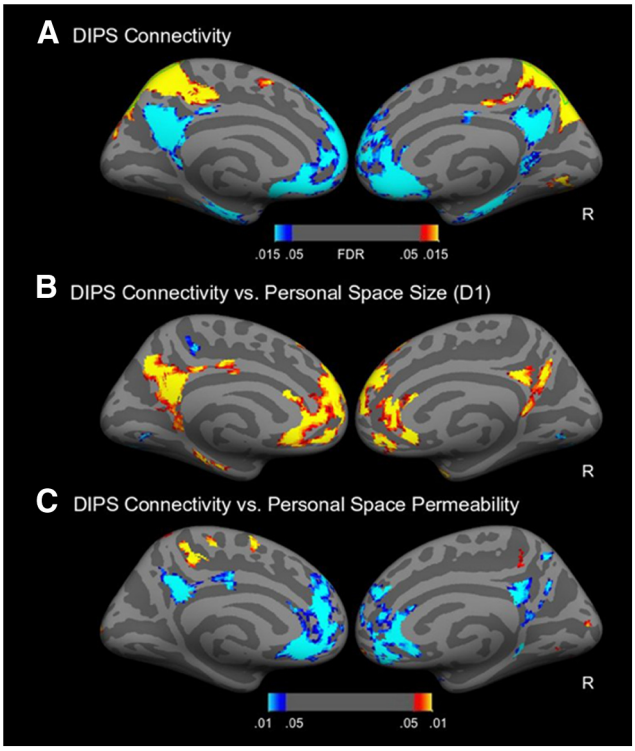

Figure 7. Correlations between DIPS-default network functional connectivity and behavior. ***A***, Medial views of the DIPS functional connectivity map (Fig. 4*A*) are shown for reference; clusters showing a significant correlation (positive, yellow-red; negative, blue) with the resting-state activity of the DIPS seed are shown. Tests for correlations between DIPS functional connectivity and behavior using voxelwise regression analyses revealed that, for regions with activity that was negatively (anti-) correlated with DIPS activity (i.e., default network regions), there were strong associations between the strength of these anti-correlations and the behavioral measures. ***B***, ***C***, Clusters of voxels showing a significant correlation (positive, yellow-red; negative, blue) between behavior (personal space size, ***B***; personal space permeability, ***C***) and that cluster's connectivity with DIPS are shown ($n = 17$). ***B***, ***C***, Functional coupling between DIPS and default network regions (including medial prefrontal cortex, mPFC, and PCC/precuneus/retrosplenial cortex) is positively correlated with personal space size (coordinates and p values for the voxel with the peak correlation: mPFC: −8, 37, 14; $p = 2 \times 10^{-6}$; PCC: 2, −51, 28; $p = 1 \times 10^{-5}$) and negatively correlated with personal space permeability (mPFC: 16, 41, 13; $p = 3 \times 10^{-6}$; PCC: −12, −41, 28; $p = 3 \times 10^{-4}$). Thus, weaker anticorrelations between DIPS and default regions (i.e., stronger connectivity) predicted larger personal space size and lower personal space permeability—a similar relationship to that found between DIPS-PMv functional connectivity and these behavioral measures (Fig. 6). R, right.

DIPS and PMv functional connectivity

We found that activity in DIPS and PMv were significantly functionally coupled, consistent with evidence for a projection between VIP and PMv in monkeys (Luppino et al., 1999). DIPS was also functionally coupled to other areas of the dorsal visual stream, such as the ventral superior parietal-occipital cortex, as well as to regions in the ventral, object-processing visual stream, such as the fusiform gyrus. This connectivity pattern suggests that DIPS may help to integrate object-related information with information about spatial location and movement of those objects (Silver and Kastner, 2009).

Personal space and social activity

In a ROI analysis, the size of personal space was negatively correlated with the strength of functional coupling between DIPS and PMv. Voxelwise regression analyses confirmed this association and showed a positive correlation between DIPS-PMv connectivity and other behavioral measures: the permeability of personal space and the amount of time the participants spent, and preferred to spend, with others. Intriguingly, permeability of personal space was positively correlated with time spent (and preferred) with others, suggesting that individual differences in personal space and social activity may be linked. Overall, these data suggest that greater DIPS-PMv functional coupling is associated with increased comfort with physical proximity to others, and higher levels of social activity.

We also found that subjects who preferred to spend more time with others showed greater approach-biased DIPS and PMv responses, suggesting that greater trait sociability is associated with stronger responsiveness, as well as functional coupling, of DIPS and PMv. It is possible that experience or learning-dependent changes in brain activity and connectivity underlie this link (Horng and Sur, 2006; Karmarkar and Dan, 2006; Lewis et al., 2009). That is, the DIPS-PMv pathway may become strengthened in an experience-dependent manner in response to social activity that involves physical proximity to others. This hypothesis is supported by previous evidence for activity-dependent plasticity of functional connectivity within frontoparietal (Albert et al., 2009) and lower-level visual (Baldassarre et al., 2012) networks, in response to motor and perceptual learning, respectively, and for associations between functional connectivity strength and social network size in humans (Bickart et al., 2012) and nonhuman primates (Sallet et al., 2011). Given that "mirror" responses of parietal and premotor areas of primate cortex have included those that represent the body parts (Ishida et al., 2010) and peripersonal space (Brozzoli et al., 2013) of nearby others, perhaps repeated stimulation of DIPS and PMv neurons with such mirroring responses during social interactions increases both stimulus-dependent and baseline (resting) neuronal activity of this pathway overall.

Clinical implications

Abnormalities in personal space regulation and dysfunction of frontoparietal networks have been reported for several neuropsychiatric conditions that are characterized by disabling impairments in social functioning, including schizophrenia (Srivastava and Mandal, 1990; Nechamkin et al., 2003; Deus and Jokić-Begić, 2006; Kang et al., 2011; Lee et al., 2014), and autism (Rudie et al., 2012; von Hofsten and Rosander, 2012) and in children or

adults with abnormal attachment patterns (Bar-Haim et al., 2002; Kaitz et al., 2004). Measurements of personal space and of related behaviors that occur during social interactions, and of the strength of neural pathways subserving these behaviors, may help clinicians detect early abnormalities in social functioning in at-risk populations. These types of measurements could permit clinicians to initiate preventative interventions before behavioral changes have developed.

References

Albert NB, Robertson EM, Miall RC (2009) The resting human brain and motor learning. Curr Biol 19:1023–1027. CrossRef Medline

Baldassarre A, Lewis CM, Committeri G, Snyder AZ, Romani GL, Corbetta M (2012) Individual variability in functional connectivity predicts performance of a perceptual task. Proc Natl Acad Sci U S A 109:3516–3521. CrossRef Medline

Bar-Haim Y, Aviezer O, Berson Y, Sagi A (2002) Attachment in infancy and personal space regulation in early adolescence. Attach Hum Dev 4:68–83. CrossRef Medline

Bickart KC, Hollenbeck MC, Barrett LF, Dickerson BC (2012) Intrinsic amygdala-cortical functional connectivity predicts social network size in humans. J Neurosci 32:14729–14741. CrossRef Medline

Bremmer F, Schlack A, Shah NJ, Zafiris O, Kubischik M, Hoffmann K, Zilles K, Fink GR (2001) Polymodal motion processing in posterior parietal and premotor cortex: a human fMRI study strongly implies equivalencies between humans and monkeys. Neuron 29:287–296. CrossRef Medline

Bremmer F, Duhamel JR, Ben Hamed S, Graf W (2002) Heading encoding in the macaque ventral intraparietal area (VIP). Eur J Neurosci 16:1554–1568. CrossRef Medline

Brozzoli C, Gentile G, Petkova VI, Ehrsson HH (2011) FMRI adaptation reveals a cortical mechanism for the coding of space near the hand. J Neurosci 31:9023–9031. CrossRef Medline

Brozzoli C, Gentile G, Bergouignan L, Ehrsson HH (2013) A shared representation of the space near oneself and others in the human premotor cortex. Curr Biol 23:1764–1768. CrossRef Medline

Buckner RL, Sepulcre J, Talukdar T, Krienen FM, Liu H, Hedden T, Andrews-Hanna JR, Sperling RA, Johnson KA (2009) Cortical hubs revealed by intrinsic functional connectivity: mapping, assessment of stability, and relation to Alzheimer's disease. J Neurosci 29:1860–1873. CrossRef Medline

Colby CL, Duhamel JR, Goldberg ME (1993) Ventral intraparietal area of the macaque: anatomic location and visual response properties. J Neurophysiol 69:902–914. Medline

Deus V, Jokić-Begić N (2006) Personal space in schizophrenic patients. Psychiatr Danub 18:150–158. Medline

Duhamel JR, Colby CL, Goldberg ME (1998) Ventral intraparietal area of the macaque: congruent visual and somatic response properties. J Neurophysiol 79:126–136. Medline

Fischl B, van der Kouwe A, Destrieux C, Halgren E, Ségonne F, Salat DH, Busa E, Seidman LJ, Goldstein J, Kennedy D, Caviness V, Makris N, Rosen B, Dale AM (2004) Automatically parcellating the human cerebral cortex. Cereb Cortex 14:11–22. CrossRef Medline

Fogassi L, Gallese V, Fadiga L, Luppino G, Matelli M, Rizzolatti G (1996) Coding of peripersonal space in inferior premotor cortex (area F4). J Neurophysiol 76:141–157. Medline

Fox MD, Snyder AZ, Vincent JL, Corbetta M, Van Essen DC, Raichle ME (2005) The human brain is intrinsically organized into dynamic, anticorrelated functional networks. Proc Natl Acad Sci U S A 102:9673–9678. CrossRef Medline

Fox MD, Corbetta M, Snyder AZ, Vincent JL, Raichle ME (2006) Spontaneous neuronal activity distinguishes human dorsal and ventral attention systems. Proc Natl Acad Sci U S A 103:10046–10051. CrossRef Medline

Graziano MS (2009) Social implications of motor control. In: The intelligent movement machine: an ethological perspective on the primate motor system, pp 1–21. Oxford: Oxford UP.

Graziano MS, Cooke DF (2006) Parieto-frontal interactions, personal space, and defensive behavior. Neuropsychologia 44:845–859. CrossRef Medline

Graziano MS, Hu XT, Gross CG (1997) Visuospatial properties of ventral premotor cortex. J Neurophysiol 77:2268–2292. Medline

Hayduk LA (1981) The permeability of personal space. Canadian J Behaval Science 13:274–287. CrossRef

Hayduk LA (1983) Personal space: where we now stand. Psychol Bull 94:293–335. CrossRef

Hill J, Inder T, Neil J, Dierker D, Harwell J, Van Essen D (2010) Similar patterns of cortical expansion during human development and evolution. Proc Natl Acad Sci U S A 107:13135–13140. CrossRef Medline

Horng SH, Sur M (2006) Visual activity and cortical rewiring: activity-dependent plasticity of cortical networks. Prog Brain Res 157:3–11. CrossRef Medline

Hosking SG, Crassini B (2010) The effects of familiar size and object trajectories on time-to-contact judgements. Exp Brain Res 203:541–552. CrossRef Medline

Ishida H, Nakajima K, Inase M, Murata A (2010) Shared mapping of own and others' bodies in visuotactile bimodal area of monkey parietal cortex. J Cogn Neurosci 22:83–96. CrossRef Medline

Kaitz M, Bar-Haim Y, Lehrer M, Grossman E (2004) Adult attachment style and interpersonal distance. Attach Hum Dev 6:285–304. CrossRef Medline

Kang SS, Sponheim SR, Chafee MV, MacDonald AW 3rd (2011) Disrupted functional connectivity for controlled visual processing as a basis for impaired spatial working memory in schizophrenia. Neuropsychologia 49:2836–2847. CrossRef Medline

Karmarkar UR, Dan Y (2006) Experience-dependent plasticity in adult visual cortex. Neuron 52:577–585. CrossRef Medline

Lee JS, Chun JW, Yoon SY, Park HJ, Kim JJ (2014) Involvement of the mirror neuron system in blunted affect in schizophrenia. Schizophr Res 152:268–274. CrossRef Medline

Lewis CM, Baldassarre A, Committeri G, Romani GL, Corbetta M (2009) Learning sculpts the spontaneous activity of the resting human brain. Proc Natl Acad Sci U S A 106:17558–17563. CrossRef Medline

Luppino G, Murata A, Govoni P, Matelli M (1999) Largely segregated parietofrontal connections linking rostral intraparietal cortex (areas AIP and VIP) and the ventral premotor cortex (areas F5 and F4). Exp Brain Res 128:181–187. CrossRef Medline

Makin TR, Holmes NP, Zohary E (2007) Is that near my hand? Multisensory representation of peripersonal space in human intraparietal sulcus. J Neurosci 27:731–740. CrossRef Medline

Nechamkin Y, Salganik I, Modai I, Ponizovsky AM (2003) Interpersonal distance in schizophrenic patients: relationship to negative syndrome. Int J Soc Psychiatry 49:166–174. CrossRef Medline

Noudoost B, Chang MH, Steinmetz NA, Moore T (2010) Top-down control of visual attention. Curr Opin Neurobiol 20:183–190. CrossRef Medline

Orban GA, Fize D, Peuskens H, Denys K, Nelissen K, Sunaert S, Todd J, Vanduffel W (2003) Similarities and differences in motion processing between the human and macaque brain: evidence from fMRI. Neuropsychologia 41:1757–1768. CrossRef Medline

Orban GA, Van Essen D, Vanduffel W (2004) Comparative mapping of higher visual areas in monkeys and humans. Trends Cogn Sci 8:315–324. CrossRef Medline

Quinlan DJ, Culham JC (2007) fMRI reveals a preference for near viewing in the human parieto-occipital cortex. Neuroimage 36:167–187. CrossRef Medline

Rudie JD, Shehzad Z, Hernandez LM, Colich NL, Bookheimer SY, Iacoboni M, Dapretto M (2012) Reduced functional integration and segregation of distributed neural systems underlying social and emotional information processing in autism spectrum disorders. Cereb Cortex 22:1025–1037. CrossRef Medline

Sallet J, Mars RB, Noonan MP, Andersson JL, O'Reilly JX, Jbabdi S, Croxson PL, Jenkinson M, Miller KL, Rushworth MF (2011) Social network size affects neural circuits in macaques. Science 334:697–700. CrossRef Medline

Schaafsma SJ, Duysens J (1996) Neurons in the ventral intraparietal area of awake macaque monkey closely resemble neurons in the dorsal part of the medial superior temporal area in their responses to optic flow patterns. J Neurophysiol 76:4056–4068. Medline

Sereno MI, Huang RS (2006) A human parietal face area contains aligned head-centered visual and tactile maps. Nat Neurosci 9:1337–1343. CrossRef Medline

Sherwood CC, Subiaul F, Zawidzki TW (2008) A natural history of the human mind: tracing evolutionary changes in brain and cognition. J Anat 212:426–454. CrossRef Medline

Silver MA, Kastner S (2009) Topographic maps in human frontal and parietal cortex. Trends Cogn Sci 13:488–495. CrossRef Medline

Srivastava P, Mandal MK (1990) Proximal spacing to facial affect expressions in schizophrenia. Compr Psychiatry 31:119–124. CrossRef Medline

Swisher JD, Halko MA, Merabet LB, McMains SA, Somers DC (2007) Visual topography of human intraparietal sulcus. J Neurosci 27:5326–5337. CrossRef Medline

Vincent JL, Kahn I, Snyder AZ, Raichle ME, Buckner RL (2008) Evidence for a frontoparietal control system revealed by intrinsic functional connectivity. J Neurophysiol 100:3328–3342. CrossRef Medline

von Hofsten C, Rosander K (2012) Perception-action in children with ASD. Front Integr Neurosci 6:115. CrossRef Medline

Yeo BT, Krienen FM, Sepulcre J, Sabuncu MR, Lashkari D, Hollinshead M, Roffman JL, Smoller JW, Zöllei L, Polimeni JR, Fischl B, Liu H, Buckner RL (2011) The organization of the human cerebral cortex estimated by intrinsic functional connectivity. J Neurophysiol 106:1125–1165. CrossRef Medline

Zar JH (1996) Biostatistical analysis. Upper Saddle River: Prentise-Hall.

Zhang T, Britten KH (2004) Clustering of selectivity for optic flow in the ventral intraparietal area. Neuroreport 15:1941–1945. CrossRef Medline